Factors controlling dissolved ^{137}Cs activities in Matsukawa-ura lagoon, a semi-closed estuary, after the Fukushima accident

Takuya Niida[1,2], Hyoe Takata[3], Sho Watanabe[4], Shinya Namura[2], Toshihiro Wada[3]

[1] Graduate School of Symbiotic Systems Science and Technology, Fukushima University, 1 Kanayagawa, Fukushima City, Fukushima 960-1296, Japan
[2] Laboratory for Instrumentation and Analysis, Environmental Engineering Division, KANSO TECHNOS CO., LTD, 3-1-1, Higashikuraji, Katano City, Osaka 576-0061, Japan
[3] Institute of Environmental Radioactivity, Fukushima University, 1 Kanayagawa, Fukushima City, Fukushima 960-1296, Japan
[4] Fukushima Prefectural Research Institute of Fisheries Resources, 1-1-14 Koyo, Soma City, Fukushima 970-0005, Japan

Correspondence to: Takuya Niida (niida_takuya@kanso.co.jp)

Abstract. The spatial and seasonal dynamics of ^{137}Cs were investigated from 2021 to 2023 in Matsukawa-ura lagoon, a semi-closed estuarine area approximately 40 km north of the Fukushima Daiichi Nuclear Power Plant (FDNPP), Japan. The weighted mean dissolved ^{137}Cs concentrations in the lagoon ranged from 5.3 to 19 Bq m^{-3}, which were 2.4−8.6 times higher than those in the surrounding coastal seawater and inflowing river waters. Furthermore, dissolved ^{137}Cs concentrations in the lagoon were higher in summer than in winter and showed a strong positive correlation with water temperature. Simplified box-model estimation indicates that continuous terrestrial input ^{137}Cs are unlikely to contribute to the spatiotemporal variability of dissolved ^{137}Cs concentrations in the lagoon. Instead ^{137}Cs deposited in bottom sediments during the early stages of the FDNPP accident is gradually released as pore waters are exposed to seawater entering the lagoon, thereby sustaining elevated dissolved ^{137}Cs concentrations. These results indicate that warmer summer conditions enhance the dissolution of ^{137}Cs from bottom sediments and highlight the importance of sediment–pore water processes in controlling ^{137}Cs dynamics in the coastal environments of Fukushima Prefecture.

1 Introduction

The Fukushima Dai-ichi Nuclear Power Plant (FDNPP) accident on 11 March 2011 released important amounts of radioactive Cs (^{134}Cs and ^{137}Cs) into the surrounding areas and the North Pacific. It is estimated that a total of 15−20 PBq of ^{137}Cs was released into the atmosphere between 12 March and 30 April 2011, with 10%–40% (2−6 PBq) estimated to have been deposited in eastern Japan (Aoyama et al., 2016). Currently, the dissolved ^{137}Cs activity concentration in seawater more than 30 km offshore Fukushima has returned to pre-accident levels (Kusakabe and Takata, 2020), whereas that in coastal waters of Fukushima Prefecture remains above pre-accident levels (Suzuki et al., 2022). Potential sources of dissolved ^{137}Cs in Fukushima coastal waters include direct inflow from the FDNPP, leaching from seabed sediments, and inflow from rivers. The completion of impermeable seaside wall in 2016 may have recently limited direct inflow from the FDNPP (Machida et al., 2019). Otosaka et al. (2020) estimated the dissolved ^{137}Cs concentrations in pore waters within bottom sediments to be 10–

40 times higher than that in the overlying water (seawater approximately 60 cm above the seafloor), suggesting that the leaching of radioactive Cs from sediments to pore water is a ^{137}Cs source in coastal areas.

Extensive studies of the riverine transport of ^{137}Cs from land to estuaries revealed that most of the ^{137}Cs transported from land to ocean is in the particulate phase (e.g., Nagao et al., 2013; Yamashiki et al., 2014; Niida et al., 2022). Although the proportion of dissolved ^{137}Cs supplied by rivers is extremely small, dissolved ^{137}Cs concentrations in the marine environment tend to be higher at near-shore sites (e.g., river mouths) than in offshore waters (Takata et al., 2020a). Accordingly, the supply from rivers to the marine environment is considered to increase dissolved ^{137}Cs concentrations. This supply is mainly regulated by water temperature and the competition between particulate-bound ^{137}Cs and ions in seawater, as described below.

Recent studies in rivers suggested that the distribution coefficient between particulate-bound ^{137}Cs and dissolved ^{137}Cs decreases with increasing water temperature, making it easier for ^{137}Cs to be released from suspended particles in rivers during the warmer summer season (Igarashi et al., 2022; Tsuji et al., 2023). Furthermore, Machida et al. (2019) estimated the ^{137}Cs export from the harbor of the FDNPP and reported higher levels in summer than in winter, indicating that the dissolved ^{137}Cs concentrations in the harbor may be related to water temperature.

Experiments reproducing the interaction between dissolved and particulate ^{137}Cs due to the flow of particulate-bound ^{137}Cs from rivers into the sea show that the distribution coefficient (K_d) between particulate-bound ^{137}Cs and dissolved ^{137}Cs decreases along a salinity gradient (Li et al., 1984; Turner, 1996). These results suggest that $^{137}Cs^+$ can be desorbed from the particles due to competition with ions such as K^+ and NH_4^+ (Takata et al., 2020b, 2021).

The relationships between water temperature and dissolved ^{137}Cs concentrations in river water and between salinity and dissolved ^{137}Cs concentrations in seawater are often discussed (Takata et al., 2022; Tsuji et al., 2023), but those in estuarine areas have not been sufficiently addressed. One of the reasons for this is that the dissolved ^{137}Cs transported from land and leached from sediments is immediately diluted and dispersed into large amounts of seawater, making quantitative assessments challenging.

This study focuses on Matsukawa-ura lagoon (Soma City, Fukushima Prefecture) and its inflowing rivers to discuss the supply of ^{137}Cs to the lagoon and the spatial and seasonal dynamics of ^{137}Cs within the lagoon. Matsukawa-ura lagoon is a semi-closed estuarine area approximately 40 km north of the FDNPP, providing an ideal area for estimating the flux of ^{137}Cs transported from rivers and desorbed from sediments. Additionally, the lagoon is only connected to the Pacific Ocean through a 100-m-wide mouth at its northmost point, facilitating the quantification of the mass balance of ^{137}Cs within the lagoon. Kambayashi et al. (2021) investigated the distribution of ^{137}Cs in Matsukawa-ura lagoon and the rivers flowing into the lagoon from 2014−2016 and calculated mass balance of ^{137}Cs, suggested that ^{137}Cs supplied from bottom sediments in the lagoon contributes greatly to the distribution of ^{137}Cs in the lagoon, with the flux supplied from bottom sediments being highest in summer. The aim of this study was to investigate the distribution of ^{137}Cs inputs, in turn allowing us to evaluate the contribution of ^{137}Cs supplied by rivers to estuarine areas, the relationships with salinity and water temperature, and the contribution and seasonality of ^{137}Cs dissolved from bottom sediments. Our results improve our understanding of radioactive contamination in aquatic habitats.

2 Material and methods

2.1 Study area and sampling stations

Matsukawa-ura lagoon is a semi-closed estuarine area with an area of 6.48 km^2 with fluctuating salinity and water temperature conditions (Wada et al., 2011; Noda et al., 2021). The lagoon has a shallow topography (mean 1.24 m depth) and a muddy sand bottom (Wada et al., 2011). Additionally, during the spring tide, about half the volume of seawater in the lagoon can be exchanged with Pacific Ocean water through the channel during a single tidal cycle because the maximum tidal amplitude is close to the mean depth of the lagoon (Kohata et al., 2003). The mean water temperature in the lagoon during 1991–2021 was 15.1 °C, with a maximum daily temperature of 28.5 °C and a minimum daily temperature of 4.5 °C (Fukushima Prefecture). Four rivers flow into Matsukawa-ura lagoon: Koizumi River (catchment area 17.8 km^2), Uda River (100.6 km^2), Ume River (10.7 km^2), and Nikkeshi River (22.6 km^2). According to the fourth aerial survey conducted by the Ministry of Education, Culture, Sports, Science and Technology, MEXT (November 2011), the mean inventory of ^{137}Cs deposited in the Koizumi, Uda, Ume, and Nikkeshi catchments were 70, 205, 70, and 93 kBq m^{-2} respectively, with relatively higher concentrations observed in the forested areas of the upstream Uda catchment. The mean concentration of ^{137}Cs across the entire Matsukawa-ura catchment was 163 kBq m^{-2} (Figure 1a). Due to the impermeable bedrock in the midstream to upstream areas of the lagoon's watershed, it is considered that precipitation hardly infiltrates the underground, instead directly flowing into the rivers and delivering 52.1% of the total precipitation runoff to the lagoon through the rivers (Kamo et al., 2014). Additionally, Arita et al. (2014) estimated the total accumulation of ^{137}Cs in surface sediments (0–20 cm depth) within the lagoon to be 220 GBq as of November 2013.

In this study, we conducted 11 samplings from June 2021 to February 2023 at 13 sites including downstream sites in the four rivers, sites at the mouths of three rivers (Koizumi, Uda, and Ume Rivers), five sites within the lagoon (from the southeast to near the lagoon mouth in the north), and a site 800 m offshore along the outer coast of the lagoon (Figure 1b). Detailed sampling locations and dates are provided in Tables S1. Table S1 presents estimated flow rates for each river on each sampling date, calculated based on the Voronoi diagram determined by the locations of Japan Meteorological Agency observation stations and assuming that 52.1% of precipitation in the 30 days prior to each sampling date flows into the rivers and 3.9 % flow into the lagoon as submarine groundwater discharge, SGD. (Kamo et al., 2014).

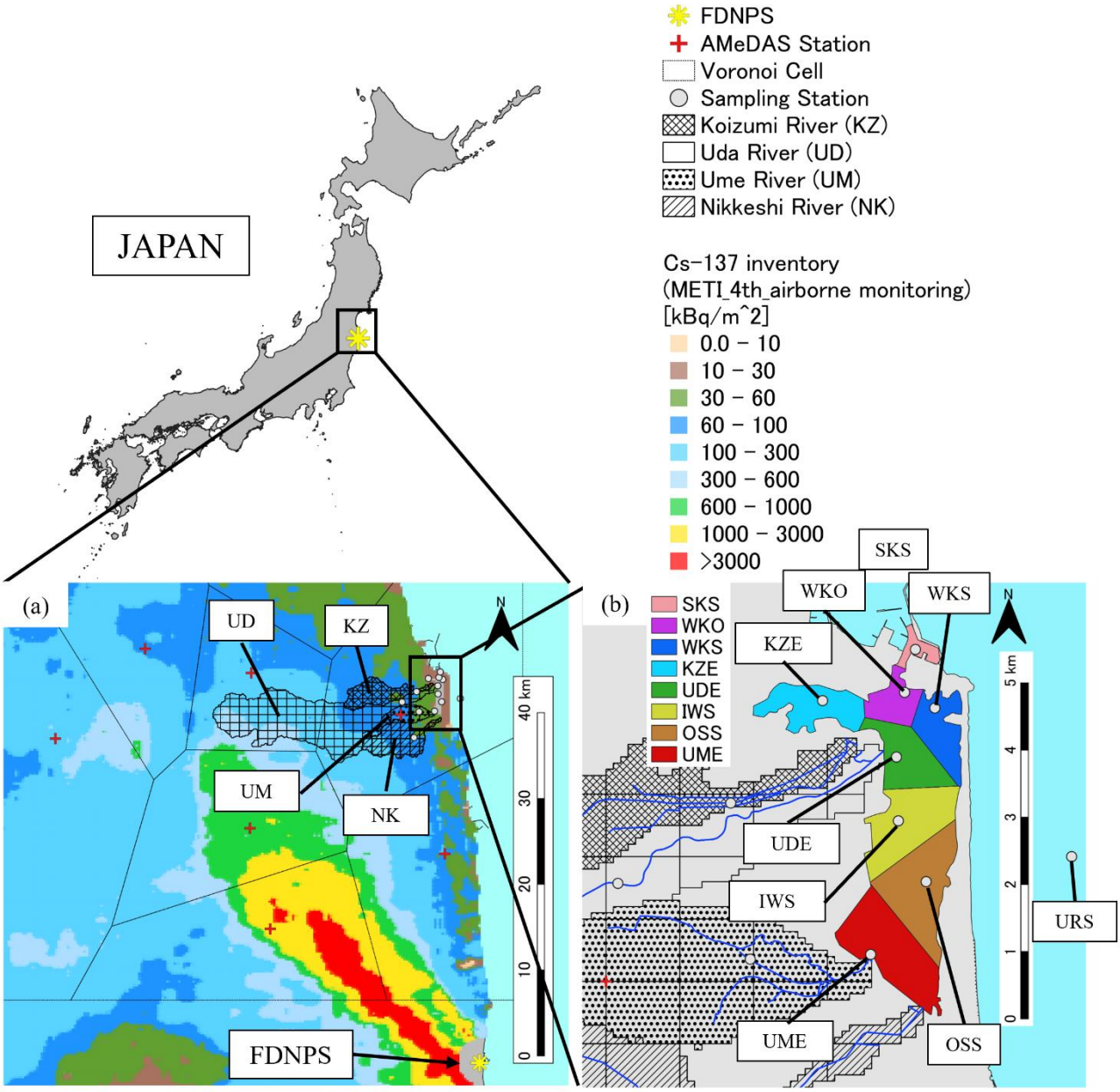

Figure 1: Spatial distribution of the ^{137}Cs inventory in the study catchment (a) and sampling stations of Matsukawa-ura lagoon (b). The spatial distribution of the ^{137}Cs inventory is based on the fourth airborne survey by MEXT (2011). The Voronoi cells were created based on the coordination of Japan Meteorological Agency weather stations (a) and sampling stations (b).

2.2 Sample processing and analysis

At each sampling site, 30–40 L of river water or surface seawater were collected using 10 L polyethylene buckets. The collected water samples were transferred to 20 L polyethylene containers and brought to the laboratory. A portion of each sample was used to measure water temperature and electrical conductivity, from which salinity was calculated. On each sampling day, the water temperature in the lagoon was measured by using a chlorophyll turbidity sensor (ACLW2-CAD, JFE Advantech Co., Ltd, Hyogo, Japan) at the station WKO, located at mouth of the lagoon, at 10:00 JST. Additionally, we measured the water depth at the station WKO from December 29, 2021. Water samples were filtered using a 0.45 μm membrane filter (047-MFPES045, AS ONE Corporation, Osaka, Japan), and approximately 20 L of the filtrate were stored for dissolved ^{137}Cs analysis. Additionally, 1–2 L of each sample were filtered through pre-weighed 0.4 μm polycarbonate filters (16040004, ADVANTEC, Tokyo, Japan) to measure the suspended particle concentration (SPc; g m^{-3}). The filters used for filtering 30–40 L of water were air-dried for about one week at 30 °C, then placed in 100 mL polyethylene containers for measurement of particle-bound ^{137}Cs concentration in suspended particles ($^{137}Cs_{sp}$; Bq kg^{-1}-dry), using a non-destructive gamma-ray spectrometer with a coaxial high-purity Ge detector (HPGe) (GEM40, SEIKO EG&G, Tokyo, Japan). The results were then divided by SPc to calculate particulate ^{137}Cs concentration ($^{137}Cs_{par}$; Bq m^{-3}). The detection limits for $^{137}Cs_{sp}$ ranged from 4.5 to 1590 Bq kg^{-1}-dry for measurement times of 80,000 s to 300,000 s, respectively. The counting efficiencies of these HPGe semiconductor detectors were calibrated using volume standard sources (MX033U8PP, The Japan Radioisotope Association, Tokyo, Japan).

To analyze dissolved ^{137}Cs concentration ($^{137}Cs_{dis}$; Bq m^{-3}), we followed the method reported by Aoyama et al. (2013), summarized here. The filtrate stored for $^{137}Cs_{dis}$ analysis was adjusted to a pH of approximately 1.6 with 15 M HNO_3. Then, 0.39 g of CsCl was added as a carrier and stirred for 2 h. Subsequently, Cs was coprecipitated with 6 g of ammonium phosphomolybdate (AMP, KANSO TECHNOS Co., LTD, Osaka, Japan). The ^{137}Cs concentration present as an impurity in the AMP was 0.05 mBq/g-AMP. The Cs-AMP precipitate was left overnight to settle, then filtered using a paper filter with a pore size of 1 μm. After air-drying the filter for about one week at 30 °C, the precipitation was enclosed in a 10 mL Teflon container, and its weight yield was determined gravimetrically. Yields exceeded 90% for all samples. The Cs-AMP compounds enclosed in the Teflon containers were measured using a non-destructive gamma-ray spectrometer with a well-type high-purity Ge detector (GWL-90-15, SEIKO EG&G, Tokyo, Japan), and the result was reported as $^{137}Cs_{dis}$. The detection limit for $^{137}Cs_{dis}$ was less than 2 Bq m^{-3} for all samples. The activity concentration of ^{137}Cs was decay-corrected to the sampling date.

Radiocerium partitioning between the dissolved and particulate phases was evaluated using the apparent distribution coefficient (*Kd*; L kg^{-1}), (IAEA, 2004). The *Kd* of ^{137}Cs is represented as follows:

$$K_d(\mathrm{L\,kg^{-1}}) = \frac{^{137}\mathrm{Cs_{sp}(Bq\,kg^{-1})}}{^{137}\mathrm{Cs_{dis}(Bq\,m^{-3})}} \times 10^3 , \quad (1)$$

2.3 Estimation of flux of dissolved ^{137}Cs in the lagoon

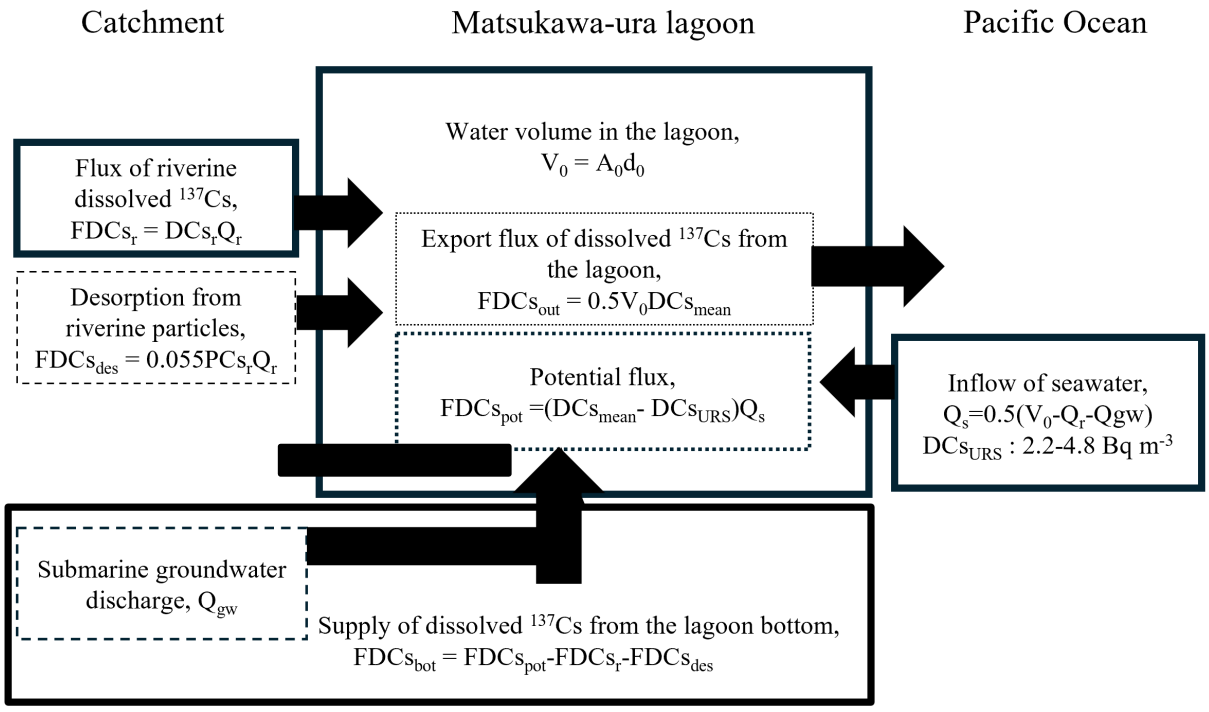

Figure 2: Schematic illustration of the box-model for water and dissolved ^{137}Cs in Matsukawa-ura Lagoon. Half of the lagoon water volume was assumed to be exchanged with coastal seawater during each tidal cycle under spring tide conditions (Kohata et al., 2003), and 5.5% of riverine particulate ^{137}Cs was assumed to be converted to dissolved ^{137}Cs through desorption after entering the lagoon (Takata et al., 2021).

We used simplified box-model estimate to evaluate the magnitudes of the internal and external sources responsible for the non-conservative mixing behavior of dissolved ^{137}Cs observed in the lagoon. ^{137}Cs budget in Matsukawa-ura lagoon is summarized in Figure 2.

The water volume in Matsukawa-ura lagoon was calculated by multiplying the area of the lagoon (6.48 km^2) by the mean water depth (1.24 m). The water volume in the lagoon was calculated using Eq. (2)

$$V_0 = A_0 d_0 = 6.48 \times 1.24 = 8.04 \,, \quad (2)$$

where V_0 is the water volume in the lagoon (Mm^3), A_0 is the area of the lagoon (km^2), d_0 is the mean depth of the lagoon (m). The maximum inflowing seawater from coastal area into the lagoon during a single tidal cycle was estimated using Eq. (3) since about half of the lagoon water volume can be exchanged with coastal seawater during a single tidal cycle under spring tide conditions (Kohata et al., 2003).

$$Q_s = 0.5(V_0 - Q_r - Q_{gw}) \,, \quad (3)$$

where Q_r is the volume of the river water discharge (m^3 12 h^{-1}), Q_{gw} is the volume of the SGD (m^3 12 h^{-1}). The values of Q_r and Q_{gw} on sampling dates are summarized in Table S1.

A Voronoi partition was constructed based on the sampling stations within the lagoon to estimate a representative dissolved ^{137}Cs concentration for the lagoon. The area ratio of each Voronoi cell to the total lagoon area was used as a weighting factor when averaging the $^{137}Cs_{dis}$ to obtain a weighted mean $^{137}Cs_{dis.}$ The weighted mean $^{137}Cs_{dis}$ (Bq m^{-3}) was estimated using Eq. (4)

$$DCs_{mean} = \frac{1}{S} \times (DCs_{SKS}A_{SKS} + DCs_{WKO}A_{WKO} + DCs_{WKS}A_{WKS} + DCs_{KZE}A_{KZE} + DCs_{UDE}A_{UDE} + DCs_{IWS}A_{IWS} + DCs_{OSS}A_{OSS} + DCs_{UME}A_{UME}), \quad (4)$$

where DCs_{mean} is the weighted mean $^{137}Cs_{dis}$ (Bq m^{-3}), A is the area of the lagoon, $DCs_{SKS\text{-}UME}$ (Bq m^{-3}) are $^{137}Cs_{dis}$ at each sampling station, $A_{SKS\text{-}UME}$ are areas of each Voronoi cell. The potential fluxes of $^{137}Cs_{dis}$ supplied to the lagoon were calculated by multiplying the difference in $^{137}Cs_{dis}$ between DCs_{mean} and coastal seawater (station URS) by the volume of seawater flowing into the lagoon. The potential fluxes of dissolved ^{137}Cs in the lagoon were calculated using Eq. (5).

$$FDCs_{pot} = (DCs_{mean} - DCs_{URS})Q_S, \quad (5)$$

where $FDCs_{pot}$ is the potential fluxes of dissolved ^{137}Cs (Bq 12 h^{-1}), DCs_{URS} is the $^{137}Cs_{dis}$ at station URS (Bq m^{-3}).

The fluxes of riverine dissolved ^{137}Cs flowing into the lagoon were calculated by multiplying the volume of river water discharge by the $^{137}Cs_{dis}$ in each river. Furthermore, 5.5% of riverine particulate ^{137}Cs was assumed to be converted to dissolved ^{137}Cs through the desorption process after flowing into the lagoon (Takata et al., 2021). The fluxes of riverine dissolved ^{137}Cs flowing into the lagoon and dissolved ^{137}Cs through the desorption process were calculated using Eqs. (6), (7) and (8).

$$FDCs_r = DCs_rQ_r, \quad (6)$$

$$FPCs_r = PCs_rQ_r, \quad (7)$$

$$FDCs_{des} = 0.055FPCs_r, \quad (8)$$

where $FDCs_r$ is the flux of riverine dissolved ^{137}Cs (Bq 12 h^{-1}), DCs_r is the riverine $^{137}Cs_{dis}$ (Bq m^{-3}), $FPCs_r$ is the flux of riverine particulate ^{137}Cs (Bq 12 h^{-1}), PCs_r is the riverine $^{137}Cs_{par}$ (Bq m^{-3}), $FDCs_{des}$ is the dissolved ^{137}Cs flux produced by desorption from riverine particulate ^{137}Cs through the desorption process (Bq 12 h^{-1}). Additionally, fluxes of dissolved ^{137}Cs supplying from the lagoon bottom were calculated using Eqs. (9). In this study, dissolved ^{137}Cs in groundwater was not measured, so the flux of dissolved ^{137}Cs from groundwater to the lagoon was not calculated.

$$FDCs_{bot} = FDCs_{pot} - FDCs_r - FDCs_{des}, \quad (9)$$

where $FDCs_{bot}$ is the flux of dissolved ^{137}Cs supplying from the lagoon bottom (Bq 12h^{-1}).

Using this assumption of a 50% water exchange per tidal cycle, the flux of dissolved ^{137}Cs exported from the lagoon to the Pacific Ocean was estimated using Eq. (10).

$$FDCs_{out} = 0.5V_0DCs_{mean}, \quad (10)$$

where $FDCs_{out}$ is the flux of the dissolved ^{137}Cs from the lagoon to the Pacific Ocean (Bq 12h^{-1}).

Each flux was normalized to a time interval of 12 h to allow for the semidiurnal tidal periodicity in the lagoon. Although the tidal prism does not fully represent the entire exchange of estuarine water with oceanic seawater entering from outside the lagoon, it is used here based on the simplified assumption that pure seawater flows in from the open ocean to help understand the monthly variation in the influx of dissolved ^{137}Cs and the key factors maintaining relatively high ^{137}Cs concentrations in the lagoon.

3 Results and discussion

3.1 ^{137}Cs concentrations in river waters

Suspended particle concentrations (SPc; g m^{-3}), particulate ^{137}Cs concentrations ($^{137}Cs_{par}$; Bq m^{-3}), ^{137}Cs concentrations in suspended particles ($^{137}Cs_{sp}$; Bq kg^{-1}-dry), dissolved ^{137}Cs concentrations ($^{137}Cs_{dis}$; Bq m^{-3}), and apparent distribution coefficients (*Kd*; L kg^{-1}) in the rivers flowing into the lagoon from 2021 to 2023 are shown in Figure 3. All riverine ^{137}Cs measurements, related parameters, and time series of $^{137}Cs_{par}$ and $^{137}C_{dis}$ are summarized in Table S2 and Figure S1.

The mean SPc were 6.7, 7.3, 14.4, and 7.5 g m^{-3} in Koizumi, Uda, Ume, and Nikkeshi Rivers, with respective median values of 2.5, 1.0, 15, and 5.4 g m^{-3} (Figure 3a). The mean values were markedly higher than the median values because samples collected during a heavy rainfall event in August 2022 increased the mean. SPc in the Ume River was relatively high compared to those in the other three rivers; this was likely due to the reduced forest floor coverage in the Ume catchment (Table S1), which is known to enhance soil erosion (Nishikiori et al., 2015). Similarly, the median $^{137}Cs_{par}$ values in the Koizumi, Uda, Ume, and Nikkeshi Rivers were 3.0, 2.0, 16, and 3.7 Bq m^{-3}, respectively (Figure 3b). Because increased SPc is associated with increased $^{137}Cs_{par}$ (Ueda et al., 2013), and both tend to increase during high-flow conditions (Nagao et al., 2013; Niida et al., 2022), the higher $^{137}Cs_{par}$ in the Ume River can be attributed to its higher SPc in the river water. The mean $^{137}Cs_{sp}$ in the Koizumi, Uda, Ume, and Nikkeshi Rivers were 1656, 1871, 2048, and 1224 Bq kg^{-1}, respectively (Figure 3c). Although the mean inventory of deposited ^{137}Cs in the Uda catchment was two to three times higher than those in the other catchments, the mean $^{137}Cs_{sp}$ in the Uda River was less than twice those in the other rivers. The mean $^{137}Cs_{dis}$ in the Koizumi, Uda, Ume, and Nikkeshi Rivers were 2.2, 1.7, 2.6, and 3.5 Bq m^{-3}, respectively (Figure 3d). The Uda River showed the lowest $^{137}Cs_{dis}$ among the four rivers, similar to the distribution reported previously (Takata et al., 2022). Previous studies reported that $^{137}Cs_{dis}$ in river water is higher in summer and lower in winter (Igarashi et al., 2022), such a seasonal trend was not observed in this study (Figure S1).

In catchments with high ^{137}Cs inventories, both $^{137}Cs_{sp}$ and the $^{137}Cs_{dis}$ in the rivers tended to be high. However, this relationship is influenced by multiple factors including topography, vegetation, rainfall patterns, and soil properties; therefore, the relationship between the ^{137}Cs concentration in soils and those in riverine particles or dissolved is not necessarily proportional. In downstream areas of catchments such as the Uda River, where soil ^{137}Cs concentrations are high in upstream areas and low in downstream areas, high $^{137}Cs_{sp}$ and $^{137}Cs_{dis}$ transported from the upstream area through the river may be diluted by downstream river waters containing less ^{137}Cs (Yamashiki et al., 2014).

K_d values ranged from 7.2×10^4 to 3.7×10^6 L kg^{-1} (Figure 3e), similar to those of rivers elsewhere in Fukushima Prefecture between 2011 and 2014, which ranged from 7.7×10^4 to 1.4×10^6 L kg^{-1} (Taniguchi et al., 2019).

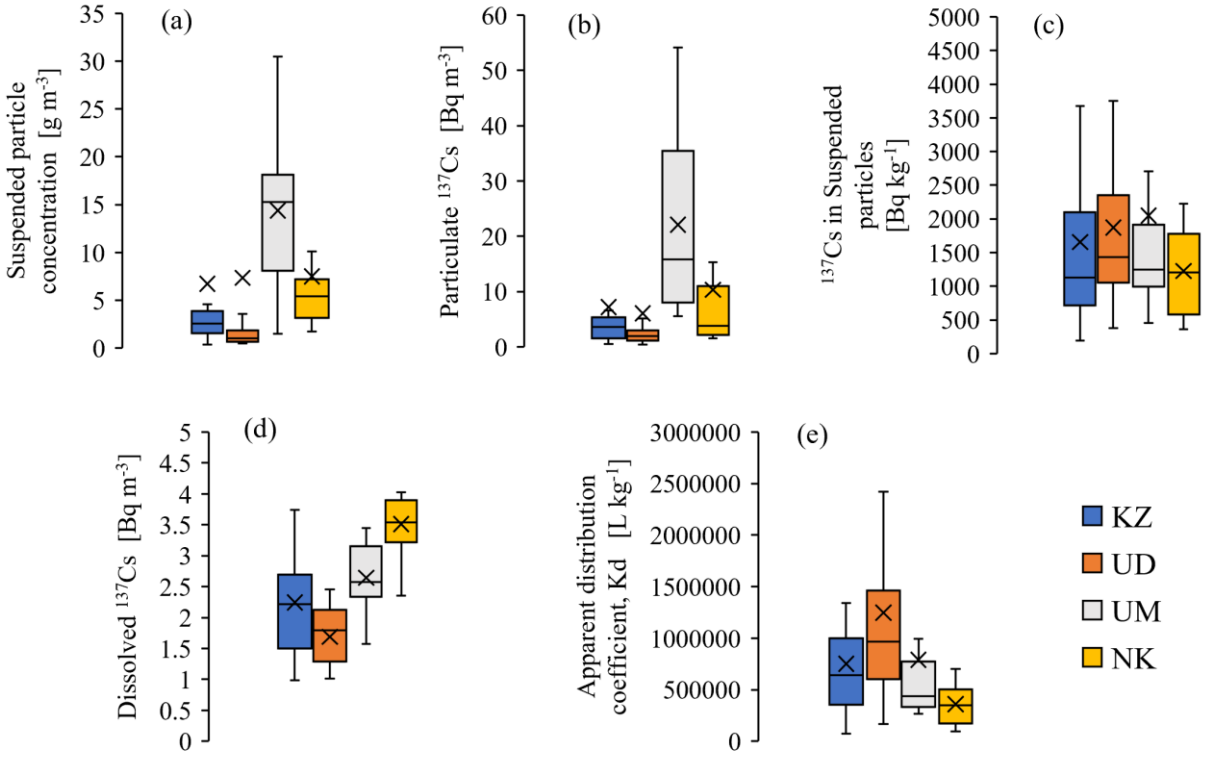

Figure 3: Water conditions in the four in flowing rivers: (a) suspended particle concentration, (b) particulate ^{137}Cs concentration, (c) ^{137}Cs concentration in suspended particles, (d) dissolved ^{137}Cs concentration, and (e) the distribution coefficient (K_d). Box plots represent the median and interquartile values, and the whiskers show the minimum and maximum values. Cross marks represent the arithmetic means of the results.

3.2 ^{137}Cs Concentrations in Matsukawa-ura Lagoon

3.2.1 Changes in parameters due to salinity

The relationships among SPc, $^{137}Cs_{par}$, $^{137}Cs_{sp}$, $^{137}Cs_{dis}$, *Kd*, and salinity in rivers, Matsukawa-ura lagoon, and the nearshore area (Station URS) are shown in Figure 4. In addition, time series of $^{137}Cs_{par}$ and $^{137}C_{dis}$ at each sampling station in the lagoon and the nearshore area are shown in Figure 5. The mean salinity in the lagoon during the study period was 29.1. All ^{137}Cs concentrations and related parameters in the lagoon and coastal seawater (station URS) are summarized in Table S3 and S4.

The mean and median SPc in the lagoon were 10.8 and 3.2 g m^{-3}, respectively (range 0.3−208 g m^{-3}). The mean and median $^{137}Cs_{par}$ were 8.1 and 2.3 Bq m^{-3}, respectively (range 0.1−123 Bq m^{-3}). The mean and median $^{137}Cs_{sp}$ were 1111 and 631 Bq kg^{-}

^{1}, respectively (range 100−16,434 Bq kg^{-1}). The mean and median $^{137}Cs_{dis}$ in the lagoon were 9.9 and 8.2 Bq m^{-3}, respectively (range 2.5−31.3 Bq m^{-3}). The K_d values tended to decrease with increasing salinity (Figure 4e). A previous study reported that SPc, $^{137}Cs_{par}$ and $^{137}Cs_{sp}$ tend to decrease with increasing salinity (Takata et al., 2022), possibly due to the dilution, coagulation, and settling of suspended particles along the salinity gradient as well as dilution by seawater with low ^{137}Cs concentrations, although no clear relationships were observed in this study (Figure 4a, b, c).

In contrast to $^{137}Cs_{par}$ and $^{137}Cs_{sp}$, $^{137}Cs_{dis}$ were higher in the lagoon than in the four inflowing rivers. $^{137}Cs_{dis}$ also tended to increase with increasing salinity (Figure 4d), reaching a maximum at salinities of 25–30, and then decreasing at salinities above 30. This trend implies that the $^{137}Cs_{dis}$ in the lagoon temporarily increases due to desorption of particulate ^{137}Cs from the rivers (Takata et al., 2020a) and the supply of dissolved ^{137}Cs from pore water in bottom sediments (Kambayashi et al., 2021; Takata et al., 2022) while it is also diluted by the large amount of coastal seawater that flows into the lagoon. However, the large variation of $^{137}Cs_{dis}$ at salinities of 25–30 (2.5−31.3 Bq m^{-3}) may be due to seasonality and differences between sampling sites. $^{137}Cs_{dis}$ tended to decrease to the north and in proximity to the mouth of the lagoon, being highest at station UME, OSS and IWS on the south side of the lagoon (Figure 1b, Figure 5f–h, respectively). The spatial pattern suggested increasing mixing with coastal seawater containing low $^{137}Cs_{dis}$ near the lagoon mouth, such as at stations WKS, WKO and SKS (Figure 1b, Figure 5b, c and e, respectively). It has been reported that some of the radiocesium adsorbed to suspended particles flowing into the ocean is desorbed from the suspended particles due to competition with ionic species such as K^+ and NH_4^+ and converted to dissolved ^{137}Cs, resulting in a decrease in K_d (Takata et al., 2020a; 2021). Similar trends were observed in this study. $^{137}Cs_{dis}$ at each station in the lagoon tended to be higher in summer and lower in winter, which contrasts with the trend observed in the rivers (Figure 5 and S1). The next section discusses the seasonal variation of $^{137}Cs_{dis}$ in the lagoon and its relationship with water temperature.

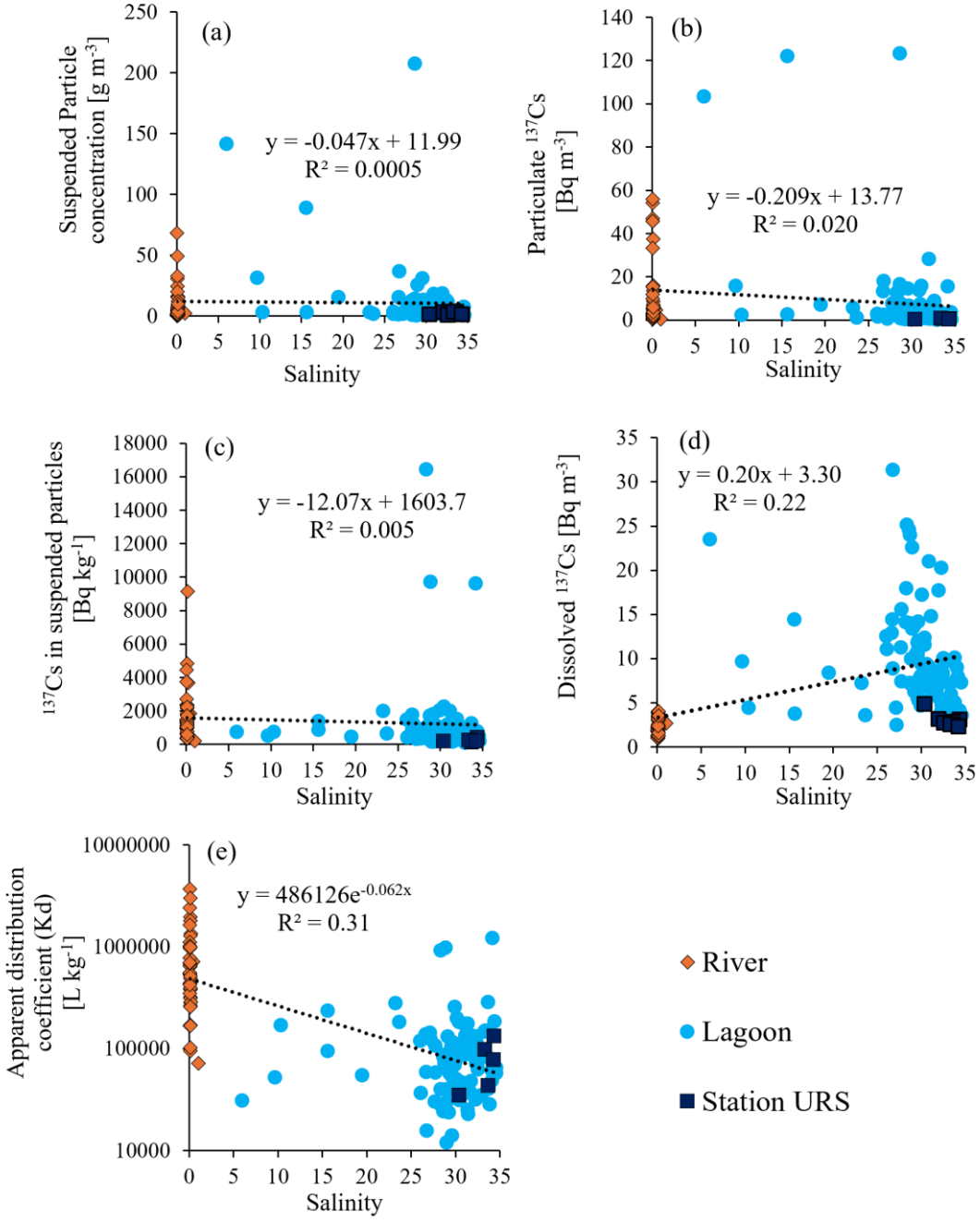

245 **Figure 4: Suspended particle concentration (a), particulate ^{137}Cs concentration (b), ^{137}Cs concentration in suspended particles (c), dissolved ^{137}Cs concentration (d), and apparent distribution coefficient (*Kd*) (e) plotted against salinity in Matsukawa-ura lagoon.**

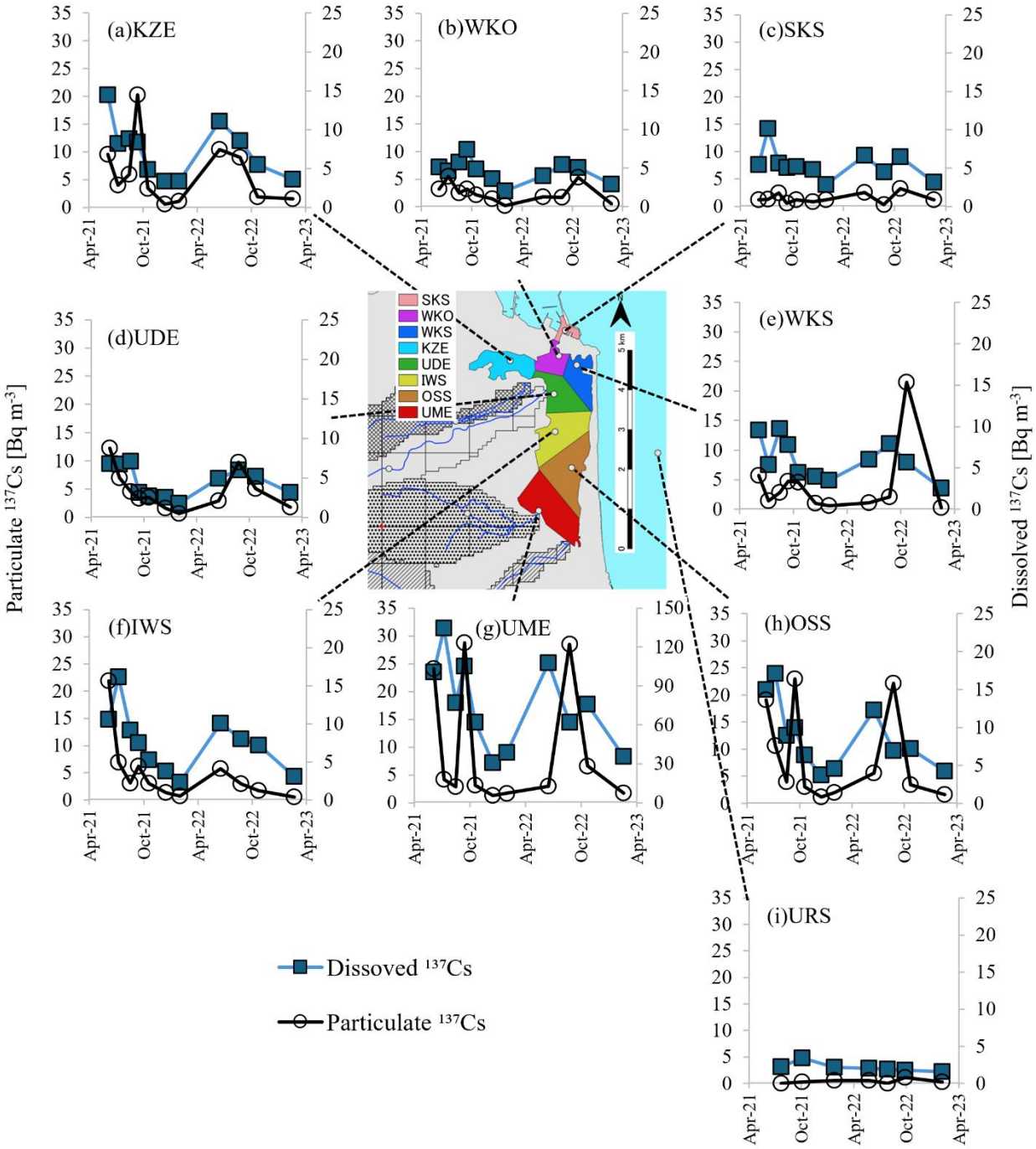

Figure 5: Time series of dissolved ^{137}Cs and particulate ^{137}Cs concentration in Matsukawa-ura lagoon. ^{137}Cs concentrations were decay-corrected to the sampling date.

3.2.2 Seasonal variation of dissolved ^{137}Cs in the lagoon

The time series of $^{137}Cs_{dis}$ in the lagoon are shown in Figure 6a and the relationship between $^{137}Cs_{dis}$ and water temperature in Figure 6b.

The weighted mean $^{137}Cs_{dis}$ in the lagoon on each sampling date ranged from 5.3−19.0 Bq m^{-3}, which is 2.4−8.6 times higher than that in coastal seawater. The corresponding values in coastal seawater ranged from 2.2−4.8 Bq m^{-3}, collected at station URS during the same period. The $^{137}Cs_{dis}$ in the lagoon tended to be higher in summer and lower in winter (Figure 6a) and showed a significant correlation with water temperature (Figure 6b). The water depth of Matsukawa-ura lagoon is very shallow, and it has been indicated that about half of the water is exchanged during a single tidal cycle under spring tide conditions (Kohata et al., 2003). For simplicity in clarifying the seasonality of $^{137}Cs_{dis}$ in the lagoon, we used the mean $^{137}Cs_{dis}$ among several sampling representative sampling stations which could represent the $^{137}Cs_{dis}$ levels in the area of the lagoon. For example, in February 2022 and 2023, $^{137}Cs_{dis}$ ranged from 2.5−9.0 and from 3.5−8.3 Bq m^{-3}, respectively, with weighted means of 5.3 and 5.5 Bq m^{-3}. In contrast, the weighted mean $^{137}Cs_{dis}$ values in June 2022 and 2023 were 17.0 and 15.0 Bq m^{-3}, respectively, which are approximately three times higher than the winter values. These results suggest that seasonal variations are more influential than spatial variability in concentrations within the lagoon.

Previous studies revealed that water temperature influences the adsorption and desorption of ^{137}Cs between solutions and particles with high affinity, such as clay minerals having “frayed-edge-sites” (FeS). Tertre et al. (2005) evaluated the effect of temperature on Cs^+ behavior at low ionic strength under neutral conditions and reported that *Kd* decreases by a factor of 3 between 25 and 150 °C. Furthermore, Igarashi et al. (2022) reported a relationship between the *Kd* value of radiocesium and water temperature in the midstream catchment of the Abukuma River, which flows through Fukushima Prefecture; they suggested that *Kd* decreases as water temperature increases. In addition, Nagao et al. (2020) reported that 0.1% of ^{137}Cs was desorbed from sand samples in ultrapure water; 3.7% in a 25% seawater solution; 7.1% in a 50% seawater solution; and 10%−12% in 100% seawater, in artificial seawater, and in a 470 mM NaCl + 8 mM KCl solution. These results indicate that the desorption of ^{137}Cs is likely to be largely completed at a salinity equivalent to that of a 50% seawater solution. In Matsukawa-ura lagoon (average salinity is 29.1), where the study was conducted, the desorption of ^{137}Cs by ion exchange in seawater was largely complete, implying that the effect of water temperature is likely more important than that of salinity in the adsorption and desorption process of ^{137}Cs in seawater.

In the following section, we apply a simplified box-model estimate approach to analyze the sources of dissolved ^{137}Cs in the lagoon and compare the contributions of river inputs against the supply from lagoon bottom.

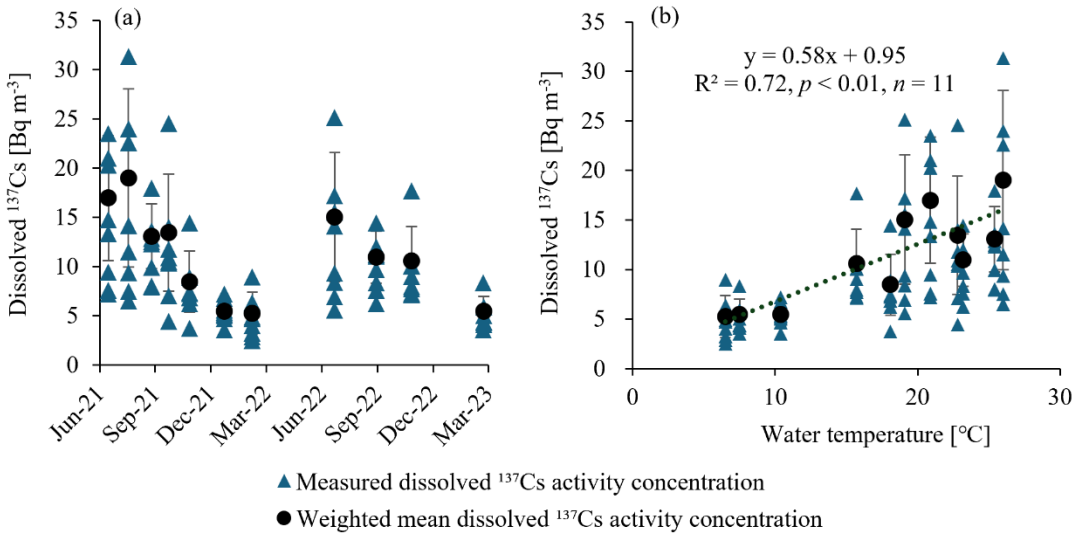

Figure 6: Time series of dissolved ^{137}Cs concentrations (a) and dissolved ^{137}Cs concentrations versus water temperature (b) in Matsukawa-ura lagoon from June 2021 to February 2023. Black bars represent the standard deviation of the dissolved ^{137}Cs concentrations on each sampling date.

3.2.3 Simplified box-model and seasonal variations in dissolved ^{137}Cs flux

The fluxes of ^{137}Cs from each river into the lagoon are shown in Figure 7. The mean fluxes of particulate ^{137}Cs from each river to the lagoon during the sampling campaign were 0.13, 0.69, 0.30 and 0.25 MBq 12 h^{-1} for Koizumi, Uda, Ume and Nikkeshi Rivers, respectively. The mean fluxes of dissolved ^{137}Cs from each river were 0.048, 0.24, 0.034 and 0.090 MBq 12 h^{-1} for Koizumi, Uda, Ume and Nikkeshi Rivers, respectively. The total flux (particulate and dissolved ^{137}Cs) from Uda Rivers, which had lower $^{137}Cs_{par}$ and $^{137}Cs_{dis}$ than the other three rivers (Figure 3(b), (d)), was nevertheless the largest among the four rivers (Figure 7c). This is because the water discharge of the Uda River is several times higher than that of the other three rivers (Table S1). The mean proportion of particulate ^{137}Cs in the total flux was about 50%−60% in all except the Ume River. However, during high-flow conditions in August 2022, particulate ^{137}Cs accounted for more than 90% of the total flux in all rivers (Figure 7d), as reported in previous studies (Nagao et al., 2013; Yamashiki et al., 2014; Niida et al., 2022). The total ^{137}Cs flux from the four rivers ranged from 0.06 to 7.24 MBq 12 h^{-1}, while the total dissolved ^{137}Cs flux ranged from 0.03 to 1.23 MBq 12 h^{-1}. In addition, assuming that 5.5% of riverine particulate ^{137}Cs is desorbed to dissolved ^{137}Cs through the desorption process after entering the lagoon (Takata et al., 2021), it was estimated that 0.003 to 0.40 MBq 12 h^{-1} was supplied to the dissolved phase by desorption from particulate ^{137}Cs.

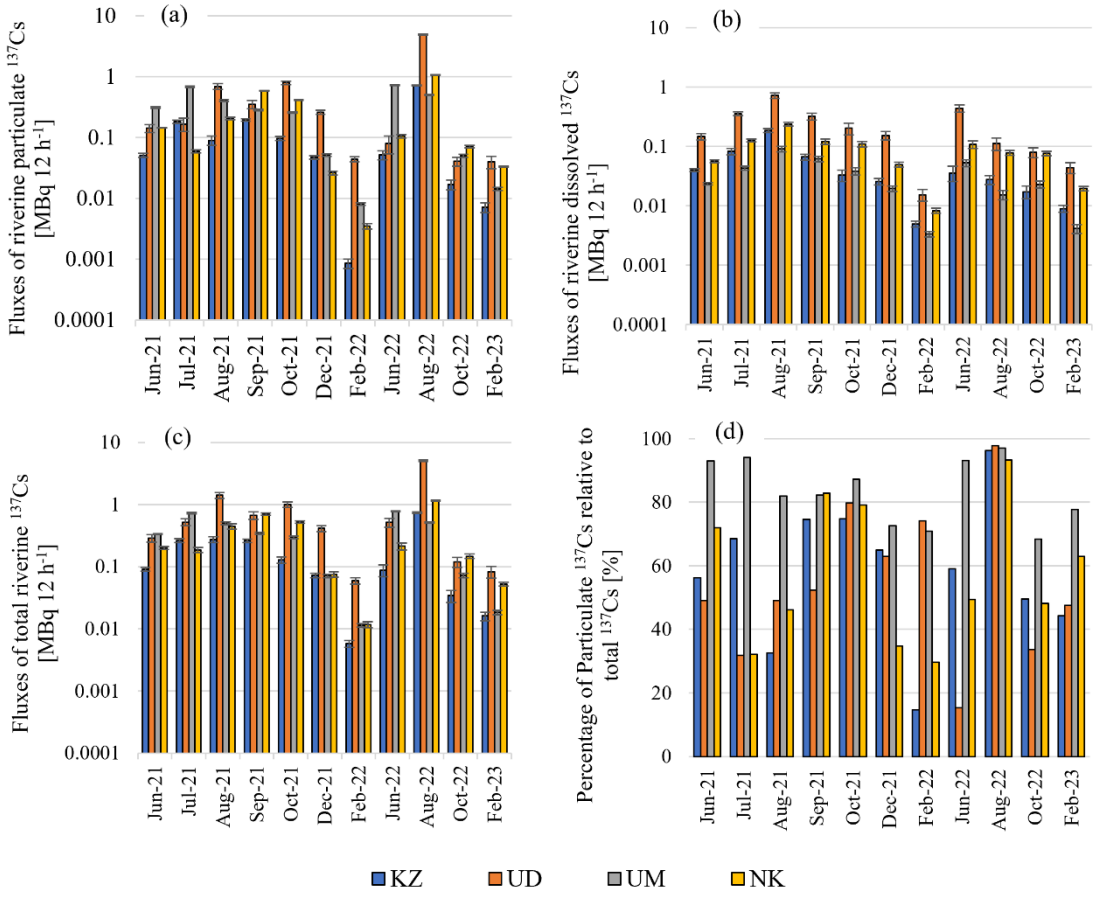

Figure 7: Fluxes of riverine particulate ^{137}Cs (a), dissolved ^{137}Cs (b) and total ^{137}Cs (c) in each river. Proportion of particulate ^{137}Cs flux in the total ^{137}Cs flux (d). Black bars represent the measurement error of ^{137}Cs.

Because the lagoon exhibits strong spatial heterogeneity in dissolved ^{137}Cs concentrations, a strict mass balance for the entire lagoon cannot be established with the present dataset. Therefore, the following calculation is intended as a simplified, first-order estimate to evaluate the relative magnitude of the major source rather than a strict mass balance. The potential fluxes of dissolved ^{137}Cs supplied to the lagoon and the flux of dissolved ^{137}Cs exported from the lagoon to the Pacific Ocean are shown in Figure 8a. Fluxes of dissolved ^{137}Cs supplied to the lagoon from the rivers, desorbed from riverine particles and supplied from the lagoon bottom are shown in Figure 8b. Details of the calculation results are shown in Table S5. The mean water depth at the station WKO, located at the mouth of the lagoon, was 1.9 m, with a maximum of 2.2 m and a minimum of 1.7 m, and the difference between the maximum and minimum values was about 50 cm (Figure S2). Therefore, the exchange volume in the lagoon was assumed to be constant throughout the year, making it possible to compare seasonal variations. The weighted

mean $^{137}Cs_{dis}$ in the lagoon during the study period was 5.3−19.0 Bq m^{-3}, whereas the $^{137}Cs_{dis}$ in the nearshore seawater outside the lagoon (station URS) during the same period was 2.2−4.8 Bq m^{-3}. This result indicates that processes within the lagoon increased $^{137}Cs_{dis}$ by up to 0.5−16.8 Bq m^{-3} after seawater entered the lagoon. Accordingly, the maximum estimated input of dissolve ^{137}Cs to the lagoon was 1.9−65.4 MBq 12 h^{-1} (Figure 8a). The fluxes of dissolved and desorbed ^{137}Cs from the rivers were 0.03−1.23 MBq $12h^{-1}$ and 0.003−0.40 MBq $12h^{-1}$, respectively, whereas the dissolved ^{137}Cs flux supplied from lagoon bottom was 1.8−64.7 MBq $12h^{-1}$, which is much greater than the riverine input. The $^{137}Cs_{dis}$ in groundwater collected in the lagoon catchment in 2015−2016 were below 9.7 Bq m^{-3} (Kambayashi et al., 2021), suggesting that the supply of dissolved ^{137}Cs via pure groundwater should be low. Therefore, the supply of dissolved ^{137}Cs from bottom sediments is likely much greater than that from rivers. These results imply that continuous ^{137}Cs input from the terrestrial areas is unlikely to contribute to the spatiotemporal variability of dissolved ^{137}Cs concentrations. Kambayashi et al. (2021) measured the ^{137}Cs concentration in pore water in sediments of Matsukawa-ura lagoon in 2016 and estimated the flux from the sediments to be 139−293 MBq day^{-1}, suggesting that the supply of dissolved ^{137}Cs from bottom sediments may account for 93−95% of the supply of $^{137}Cs_{dis}$ to Matsukawa-ura lagoon. However, our estimates show that the supply of dissolved ^{137}Cs from lagoon bottom may account for more than 96%. Thus, as more time passes since the accident and riverine inputs of ^{137}Cs decrease due to decontamination in the catchments, the relative contribution from bottom sediments is expected to increase.

The supply of dissolved ^{137}Cs from bottom sediments was higher in summer and lower in winter (Figure 8b), consistent with the seasonal variation in $^{137}Cs_{dis}$ in the lagoon. This seasonal pattern may be attributed to a decrease in the distribution coefficient between particulate and dissolved ^{137}Cs with increasing water temperature (Tertre et al., 2005), as discussed in Section 3.2.2. In addition, Tsuji et al. (2022) investigated the effects of water temperature, dissolved oxygen, and NH_4^+ on the desorption of ^{137}Cs from lake sediments at Yokokawa Dam, Fukushima Prefecture, and reported that higher water temperatures stimulate bacterial decomposition of organic matter, while elevated NH_4^+ concentrations in pore water under anaerobic conditions enhance the desorption of ^{137}Cs from mineral particles. Because ^{137}Cs bound to clay minerals is more readily exchanged with NH_4^+ than with K^+ (Wauters et al., 1997), not only the temperature-dependent decrease in the distribution coefficient but also the production of NH_4^+ under warm and anaerobic summer conditions may promote the desorption of ^{137}Cs from bottom sediments in coastal environments, thereby supplying ^{137}Cs to the overlying seawater by tidal pumping.

In this study, the fluxes of dissolved ^{137}Cs supplied to the lagoon from rivers and bottom sediments were estimated to be 14.3−65.4 MBq $12h^{-1}$ from June to October and 1.9−13.1 MBq $12h^{-1}$ from December to February. Niida et al. (2022) estimated the fluxes of ^{137}Cs exported to the Pacific Ocean during July 27−29, 2020, when the total rainfall was approximately 80 mm, were 107, 120 and 109 MBq in the Niida, Ukedo and Takase River catchment. These rivers and their catchments are located closer to FDNPP than Matsukawa-ura and have a much higher ^{137}Cs inventories (853, 2359, and 701 kBq m^{-2}). These fluxes are comparable to the estimated daily flux of dissolved ^{137}Cs exported from Matsukawa-ura into the Pacific Ocean during summer. In contrast, based on the results of a survey conducted by Naulier et al. (2017) in October 2014, the fluxes of dissolved

^{137}Cs exporting to the Pacific Ocean from Mano, Niida, and Ota River, which are located in northern Fukushima Prefecture, were calculated to be 10.7, 15.1, and 9.3 MBq 12h^{-1}, respectively. These comparisons indicate that the impact of dissolved ^{137}Cs export from Matsukawa-ura lagoon to coastal waters is relatively large in summer. Based on our results, we conclude that ^{137}Cs in bottom sediments, deposited during the early stages of FDNPP accident, gradually dissolves when pore waters are exposed to seawater entering the lagoon, and that warmer seawater temperatures during the summer may further accelerate the dissolution process. This mechanism likely plays an important role in the spatiotemporal redistribution of ^{137}Cs in the coastal waters of Fukushima Prefecture.

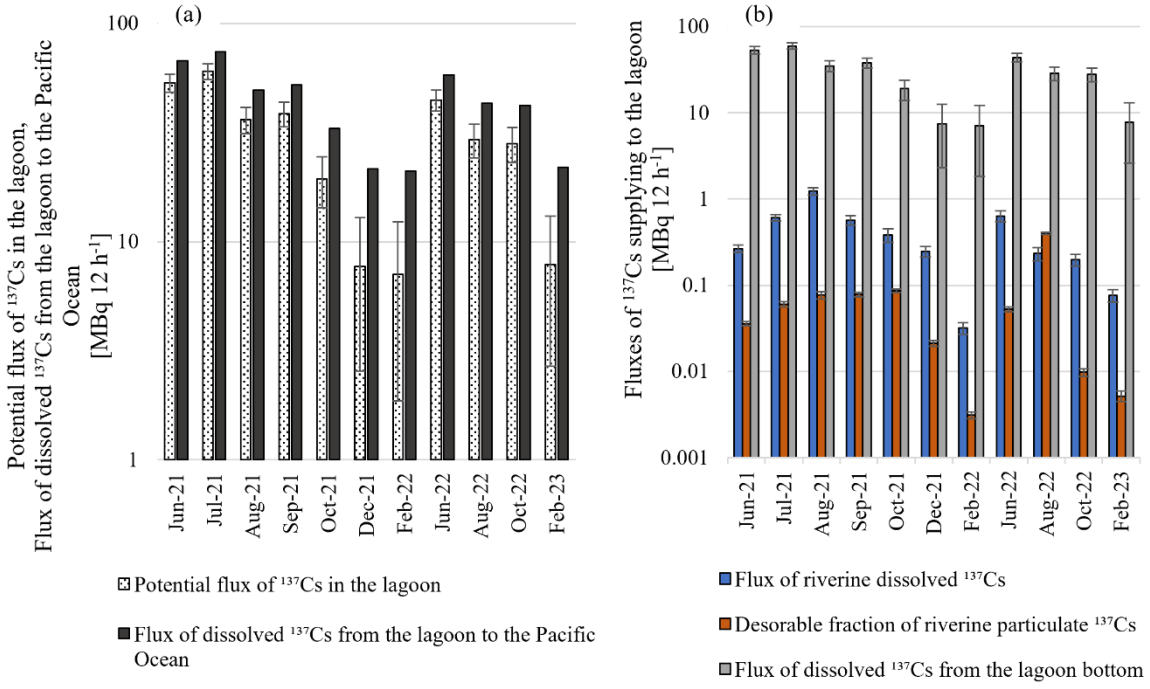

Figure 8: Potential fluxes of dissolved ^{137}Cs supplied to Matsukawa-ura lagoon and fluxes of dissolved ^{137}Cs from the lagoon to the Pacific Ocean (a). Fluxes of dissolved ^{137}Cs supplied to the lagoon from the rivers, desorbed from riverine particles and the lagoon bottom in the lagoon (b). Black bars represent the measurement error of ^{137}Cs.

4 Conclusion

We investigated the spatial and seasonal dynamics of ^{137}Cs in Matsukawa-ura lagoon, a semi-enclosed estuarine system located approximately 40 km north of the Fukushima Daiichi Nuclear Power Plant, Japan. Dissolved ^{137}Cs concentrations in the lagoon were higher than those in river water flowing into the lagoon and in adjacent coastal seawater, indicating the

influence of desorption from suspended sediments associated with increasing salinity. In addition, dissolved ^{137}Cs concentrations in the lagoon were higher in summer and lower in winter, demonstrating a clear influence of water temperature.

Quantification of source contributions using a simplified box-model estimate approach revealed that the supply of dissolved ^{137}Cs from bottom sediments was much greater than that from rivers and suspended sediments. These results indicate that continuous terrestrial inputs of ^{137}Cs are unlikely to control the spatiotemporal variability of dissolved ^{137}Cs concentrations in the lagoon. Instead, we conclude that ^{137}Cs deposited in bottom sediments during the early stage of the Fukushima Daiichi Nuclear Power Plant accident is gradually released as pore waters are exposed to seawater entering the lagoon. Moreover, higher summer seawater temperatures likely accelerate the release of ^{137}Cs from bottom sediments.

The daily flux of dissolved ^{137}Cs exported from Matsukawa-ura lagoon to the Pacific Ocean during summer is comparable to the flux exported from major rivers in Fukushima Prefecture under high-flow conditions. This finding indicates that, to better understand the causes of elevated dissolved ^{137}Cs concentrations in coastal waters of Fukushima Prefecture, it is essential to strengthen monitoring of bottom sediments and pore waters, particularly in estuaries and coastal areas, in order to clarify the dynamics and impacts of ^{137}Cs released from sediments. Future studies should further investigate the relationships between ^{137}Cs concentrations in bottom sediments and pore waters in estuarine and coastal environments, with particular attention to seasonal variations in water temperature as well as water quality.

Team list

Corresponding Author

Takuya Niida – *Graduate School of Symbiotic Systems Science and Technology, Fukushima University, 1 Kanayagawa, Fukushima City, Fukushima 960-1296, Japan;* Email (present): s2571005@ipc.fukushima-u.ac.jp

Laboratory for Instrumentation and Analysis, Environmental Engineering Division, KANSO TECHNOS CO., LTD, 3-1-1, Higashikuraji, Katano City, Osaka 576-0061, Japan; Phone: +81-72-810-6551; Email (permanent): niida_takuya@kanso.co.jp

Authors

Hyoe Takata - *Institute of Environmental Radioactivity, Fukushima University, 1 Kanayagawa, Fukushima City, Fukushima 960-1296, Japan;* Email: h.takata@ier.fukushima-u.ac.jp

Sho Watanabe - *Fukushima Prefectural Research Institute of Fisheries Resources, 1-1-14 Koyo, Soma City, Fukushima 970-0005, Japan;* Email: watanabe_shou_01@pref.fukushima.lg.jp

Shinya Namura - *Laboratory for Instrumentation and Analysis, Environmental Engineering Division, KANSO TECHNOS CO., LTD, 3-1-1, Higashikuraji, Katano City, Osaka 576-0061, Japan;* Email: namura_shinya@kanso.co.jp

Toshihiro Wada - *Institute of Environmental Radioactivity, Fukushima University, 1 Kanayagawa, Fukushima City, Fukushima 960-1296, Japan;* Email: t-wada@ipc.fukushima-u.ac.jp

Author contribution

The manuscript was written through contributions of all authors. All authors have given approval to the final version of the manuscript.

Competing interest

The authors declare that they have no conflict of interest.

Acknowledgements

We are grateful to researchers of the Fukushima Prefectural Research Institute of Fisheries Resources for their cooperation during sampling.

Financial support

This research is an achievement of " Stabilizing resources through effective release of seedlings using ICT infrastructure" (JPFR23060109, JPFR24060109, JPFR25060109) among advanced technology development projects in the field of agriculture, forestry and fisheries. (Fukushima Institute for Research, Education and Innovation (F-REI)).

References

Aoyama, M.; Uematsu, M.; Tsumune, M.; Hamajima, Y.: Surface pathway of radioactive plume of TEPCO Fukushima NPP1 released ^{134}Cs and ^{137}Cs. Biogeosciences., 10, 3067-3078. https://doi.org/10.5194/bg-10-3067-2013, 2013.

Aoyama, M.; Kajino, M.; Tanaka, T.Y.; Sekiyama, T.T.; Tsumune, D.; Tsubono, T.; Hamajima, Y.; Inomata, Y.; Gamo, T. :^{134}Cs and ^{137}Cs in the North Pacific Ocean derived from the TEPCO Fukushima Dai-ichi Nuclear Power Plant accident, Japan in March 2011. Part Two: estimation of ^{134}Cs and ^{137}Csinventories in the North Pacific Ocean. J. Oceanogr., 72, 67-76. https://doi.org/10.1007/s10872-015-0332-2, 2016.

Arita, K.; Yabe, T.; Hayashi, S.: Actual situation of concentration and inventory of radioactive cesium in Matsukawa-ura Lagoon sediment, Fukushima Prefecture. J. Jpn. Soc. Civ. Eng.Ser. G (Environ. Res.)., 70, III_225–III_231 (in Japanese with English abstract). https://doi.org/10.2208/jscejer.70.III_225, 2014.

Fukushima prefecture Website; https://www.pref.fukushima.lg.jp/sec/37380b/suion.html. (Accessed 30 June 2024).

IAEA, 2004. Sediment Distribution Coefficients and Concentration Factors for Biota in the Marine Environment. Technical Reports Series No. 422.

Igarashi, Y.; Nanba, K.; Wada, T.; Wakiyama, Y.; Onda, Y.; Moritaka, S.; Konoplev, A.: Factors controlling the dissolved ^{137}Cs seasonal fluctuations in the Abukuma river under the influence of the Fukushima nuclear power plant accident. J. Geophys. Res.: Biogeosci., 127 (1), e2021JG006591. https://doi.org/10.1029/2021JG006591, 2022.

Japan Atomic Energy Agency Web site; Results of the Fourth Airborne Monitoring Survey by MEXT. https://emdb.jaea.go.jp/emdb_old/portals/b1020201/. (Accessed 15 April 2024).

Kambayashi, S.; Zhang, J.; Narita, H.: Significance of Fukushima-derived radiocaesium flux via river-estuary-ocean system. Sci. Total Environ., 793, 148456. https://doi.org/10.1016/j.scitotenv.2021.148456, 2021.

Kamo, T.; Suzuki, M.; Wada, T.; Iwasaki, T.; Watanabe, T.; Nishi, R.; Tsurunari, Y.: Estimation of freshwater discharge and field observation on aquatic environment around the entrance of Matsukawaura inlet. J. Jpn. Soc. Civ. Eng. Ser. B3 Ocean. Eng., 70, I_1020–I_1025 (in Japanese with English abstract). https://doi.org/10.2208/jscejoe.70.I_1020, 2014.

Kohata, K.; Hiwatari, T.; Hagiwara, T. Natural water-purification system observed in a shallow coastal lagoon: Matsukawa-ura, Japan. Mar. Pollut. Bull., 47, 148-154. https://doi.org/10.1016/S0025-326X(03)00055-9, 2003.

Kusakabe, M.; Takata, H.: Temporal trends of ^{137}Cs concentration in seawaters and bottom sediments in coastal waters around Japan: implications for the Kd concept in the dynamic marine environment. J. Radioanal. Nucl. Chem., 323, 567–580. https://doi.org/10.1007/s10967-019-06958-z, 2020.

Li, Y.-H.; Burkhardt, L.; Teraoka, H.: Desorption and coagulation of trace elements during estuarine mixing. Geochim. Cosmochim. Acta., 48, 1879–1884. https://doi.org/10.1016/0016-7037(84)90371-5, 1984.

Machida, M.; Yamada, S.; Iwata, A.; Otosaka, S.; Kobayashi, T.; Watanabe, M.; Funasaka, H.; Morita, T.: Seven-year temporal variation of Cesium-137 discharge inventory from the port of Fukushima Dai-ichi Nuclear Power Plant. Trans. At. Energy Soc. Japan., 18, 226–236 (in Japanese with English abstract). https://doi.org/10.3327/taesj.J18.030, 2019.

Moore, W.S.; The subterranean estuary: a reaction zone of ground water and sea water. Mar. Chem., 65, 111-125. https://doi.org/10.1016/S0304-4203(99)00014-6, 1999.

Moore, W.S.; The effect of submarine groundwater discharge on the ocean. Annu Rev. Mar. Sci., 2:59-88. https://doi.org/10.1146/annurev-marine-120308-081019, 2010.

Nagao, S.; Kanamori, M.; Ochiai, S.; Tomihara, S.; Fukushi, K.; Yamamoto, M.: Export of ^{134}Cs and ^{137}Cs in the Fukushima river systems at heavy rains by Typhoon Roke in September 2011. Biogeosci. Discuss., 10, 6212-6223. https://doi.org/10.5194/bg-10-6215-2013, 2013.

Nagao, S.; Terasaki, S.; Ochiai, S.; Fukushi, K.; Tomihara, S.; Charette, M. A.; Buesseler, K. O.: Desorption Behavior of Fukushima-derived Radiocesium in Sand Collected from Yotsukura Beach in Fukushima Prefecture. Anal. Sci., 36, 569-573. https://doi.org/10.2116/analsci.19SBP08, 2020.

Naulier, M.; Eyrolle-Boyer, F.; Boyer P.; Metivier, J.M.; Onda, Y.: Particulate organic matter in rivers of Fukushima: An unexpected carrier phase for radiocesiums. Sci. Total Environ, 579, 1560-1571. http://dx.doi.org/10.1016/j.scitotenv.2016.11.165, 2017.

Niida, T.; Wakiyama, Y.; Takata, H.; Taniguchi, K.; Kurosawa, H.; Fujita, K.; Konoplev, A.: A comparative study of riverine ^{137}Cs dynamics during highflow events at three contaminated river catchments in Fukushima. Sci. Total Environ., 821, 153408. https://doi.org/10.1016/j.scitotenv.2022.153408, 2022.

Nishikiori, T.; Ito, S.; Tsuji, H.; Yasutaka, T.; Hayashi, S.: Influence of Forest Floor Covering on Radiocesium Wash-off Associated with Forest Soil Erosion. J. Jpn. For. Soc., 97, 63―69 (in Japanese with English abstract). https://doi.org/10.4005/jjfs.97.63, 2015.

Noda, T.; Wada, T.; Mitamura, H.; Kume, M.; Komaki, T.; Fujita, T.; Sato, T.; Narita, K.; Yamada, M.; Matsumoto, A.; Hori, T.; Takagi, J.; Kutzer, A.; Arai, N.; Yamashita, Y.: Migration, residency and habitat utilisation by wild and cultured Japanese eels (Anguilla japonica) in a shallow brackish lagoon and inflowing rivers using acoustic telemetry. J. Fish Biol., 98, 507–525. https://doi.org/10.1111/jfb.14595, 2021.

Otosaka, S.; Kambayashi, S.; Fukuda, M.; Tsuruta, T.; Misonou, T.; Suzuki, T.; Aono, T.: Behavior of radiocesium in sediments in Fukushima coastal waters: verification of desorption potential through pore water. Environ. Sci. Technol., 54, 13778–13785. https://doi.org/10.1021/acs.est.0c05450, 2020.

Sanial, V.; Buesseler, K.O.; Charette, M.A.; Nagao, S.: Unexpected source of Fukushima-derived radiocesium to the coastal ocean of Japan. PNAS., 114(42), 11092–11096. https://doi.org/10.1073/pnas.1708659114, 2017.

Suzuki, S.; Amano, Y.; Enomoto, M.; Matsumoto, A.; Morioka, Y.; Sakuma, K.; Tsuruta, T.; Kaeriyama, H.; Miura, H.; Tsumune, D.; Kamiyama, K.; Wada, T.; Takata, H.: Temporal variability of ^{137}Cs concentrations in coastal sediments off Fukushima. Sci. Total Environ., 831, 154670. https://doi.org/10.1016/j.scitotenv.2022.154670, 2022.

Takata, H.; Aono, T.; Aoyama, M.; Inoue, M.; Kaeriyama, H.; Suzuki, S.; Tsuruta, T.; Wada, T.; Wakiyama, Y.: Suspended particle–water interactions increase dissolved ^{137}Cs activities in the nearshore seawater during typhoon Hagibis. Environ. Sci. Technol., 54, 10678–10687. https://doi.org/10.1021/acs.est.0c03254, 2020a.

Takata, H.; Inatomi, N.; Kudo, N.: The contribution of ^{137}Cs export flux from the Tone River Japan to the marine environment. Sci. Total Environ., 701, 134550. https://doi.org/10.1016/j.scitotenv.2019.134550, 2020b.

Takata, H.; Wakiyama, Y.; Niida, T.; Igarashi, Y.; Konoplev, A.; Inatomi, N.: Importance of desorption process from Abukuma River's suspended particles in increasing dissolved ^{137}Cs in coastal water during river-flood caused by typhoons. Chemosphere., 281, 130751. https://doi.org/10.1016/j.chemosphere.2021.130751, 2021.

Takata, H.; Wada, T.; Aono, T.; Inoue, M.; Kanasashi, T.; Suzuki, S.; Amano, Y.: Factors controlling dissolved ^{137}Cs activities in coastal waters on the eastern and western sides of Honshu, Japan, Environ, Sci. Total Environ., 806, 151216. https://doi.org/10.1016/j.scitotenv.2021.151216, 2022.

Taniguchi, K.; Onda, Y.; Smith, H.G.; Blake, W.; Yoshimura, K.; Yamashiki, Y.; Kuramoto, T.; Saito, K.: Transport and redistribution of radiocaesium in Fukushima fallout through rivers. Environ. Sci. Technol., 53, 12339–12347. https://doi.org/10.1021/acs.est.9b02890, 2019.

Tertre, E.; Berger, G.; Castet, S.; Loubet, M.; Giffaut, E.: Experimental sorption of Ni_2^+, Cs^+ and Ln_3^+ onto a montmorillonite up to 150°C. Geochim. Cosmochim. Acta., 69(21), 4937–4948. https://doi.org/10.1016/j.gca.2005.04.024, 2005.

Tsuji, H.; Funaki, H.; Watanabe, M.; Hayashi, S.: Effects of temperature and oxygen on ^{137}Cs desorption from bottom sediment of a dam lake. Appl. Geochem., 140, 105303. https://doi.org/10.1016/j.apgeochem.2022.105303, 2022.

Tsuji, H.; Nishikiori, T.; Ito, S.; Ozaki, H.; Watanabe, M.; Sakai, M.; Ishii, Y.; Hayashi, S.: Influential factors of long-term and seasonal ^{137}Cs change in agricultural and forested rivers: Temperature, water quality and an intense Typhoon Event. Environ. Pollut., 338, 122617. https://doi.org/10.1016/j.envpol.2023.122617, 2023.

Turner, A.: Trace-metal partitioning in estuaries: importance of salinity and particle concentration. Mar. Chem., 54, 27–39. https://doi.org/10.1016/0304-4203(96)00025-4, 1996.

Ueda, S.; Hasegawa, H.; Kakiuchi, H.; Akata, N.; Ohtsuka, Y.: Fluvial discharges of radiocaesium from watersheds contaminated by the Fukushima Dai-ichi Nuclear Power Plant accident, Japan. J. Environ. Radioact., 118, 96-104. https://doi.org/10.1016/j.jenvrad.2012.11.009, 2013.

Wada, T.; Kamiyama, K.; Shimamura, S.; Matsumoto, I.; Mizuno, T.; Nemoto, Y.: Habitat utilization, feeding, and growth of wild spotted halibut Verasper variegatus in a shallow brackish lagoon: Matsukawa-ura, northeastern Japan. Fish. Sci., 77, 785–793. https://doi.org/10.1007/s12562-011-0385-0, 2011.

Yamashiki, Y.; Onda, Y.; Smith, H.G.; Blake, W.H.; Wakahara, T.; Igarashi, Y.; Matsuura, Y.; Yoshimura, K.: Initial flux of sediment-associated radiocesium to the ocean from the largest river impacted by Fukushima Daiichi Nuclear Power Plant. Sci. Rep., 4, 3714. https://doi.org/10.1038/srep03714, 2014.